Energy levels of Co^{2+} in CoF_2 and $CsCoCl_3$

1995 J. Phys.: Condens. Matter 7 2917

(http://iopscience.iop.org/0953-8984/7/14/028)

J. Phys.: Condens. Matter 7 (1995) 2917–2929. Printed in the UK

Energy levels of Co^{2+} in CoF_2 and $CsCoCl_3$

T Nguyen, S E Nagler†, R A Cowley, T Perring‡ and R Osborn§
Oxford Physics, Clarendon Laboratory, Parks Road, Oxford OX1 3PU, UK

Received 15 November 1994

Abstract. Neutron scattering measurements have been made of the high-energy excitonic excitations of Co^{2+} ions in CoF_2 and $CsCoCl_3$. The measurements were performed with the HET direct geometry time-of-flight spectrometer on the ISIS pulsed neutron source at the Rutherford Appleton Laboratory. In the case of CoF_2 the results are consistent with previous estimates of the crystal-field and spin–orbit parameters, but for $CsCoCl_3$ there are marked discrepancies. The results can be fitted by adjusting the crystal-field parameters, but this has the consequence that the exchange interactions between the spins in $CsCoCl_3$ are anisotropic.

1. Introduction

Cobalt ions are unusual 3d transition metal ions because the orbital angular momentum of the electrons is often not wholly quenched by the crystal field. Consequently, there are a number of energy levels that have different angular momentum, and whose properties depend on the local environment, spin–orbit interaction and magnetic ordering. The development of pulsed neutron spallation sources has made it possible to study high-energy electronic excitations with neutron scattering, and these techniques have been successfully applied to the crystal-field levels in the rare-earth metals and in the actinides (Osborn *et al* 1991). The present experiment describes the extension of this work to the 3d transition metal ions. The experiments were performed using the time-of-flight direct-geometry spectrometer HET on the ISIS pulsed neutron source at the Rutherford Appleton Laboratory, and are described in detail in section 3.

The materials chosen for the study were CoF_2 and $CsCoCl_3$. The energy levels of Co ions in the rutile structure of CoF_2 were first studied by optical and spin-resonance techniques as applied to dilute Co ions in MgF_2 by Johnston *et al* (1964) and by Gladney (1966). The three excitations of lowest energy of CoF_2 were then studied with neutron scattering techniques by Martel *et al* (1968), and the results analysed to give the crystal-field and spin–orbit parameters by Cowley *et al* (1973). The higher-energy excitations could not at that time be studied with neutron scattering techniques but, as shown in section 3, can now be observed.

$CsCoCl_3$ is of considerable interest because the magnetic excitations are a good model for a quasi-one-dimensional, $S = 1/2$, antiferromagnet with nearly Ising-like interactions and detailed studies of the low-energy spin excitations have been made with neutron scattering techniques by Tellenbach and Arend (1977), Yoshizawa *et al* (1981) and by

† Permanent address: Department of Physics, University of Florida, Gainsville, FL, USA.
‡ Permanent address: Argonne National Laboratory, Argonne, IL, USA.
§ Permanent address: Rutherford Appleton Laboratory, Chilton, Didcot, Oxfordshire, UK.

0953-8984/95/142917+13$19.50

Nagler *et al* (1983). A quantitative account of these results requires a detailed knowledge of the low-lying electronic states of the Co ions, because they can be mixed into the ground state.

Unfortunately, it has not been proved from optical measurements on $CsCoCl_3$ using Raman scattering techniques (Johnstone and Dubicki 1980, Johnstone *et al* 1982) to determine the energies conclusively, and so further evidence is presented in section 3 and analysed in section 4.

The layout of the paper is such that the crystal-field theory of the Co^{2+} ions is described in section 2, and the experiments and the results are given in section 3, while the conclusions are presented in section 4.

2. Theory of the electronic excitations of co ions

2.1. The energy levels

Both CoF_2 and $CsCoCl_3$ have the ions surrounded by a distorted octahedron of either F ions (Stout and Reed 1954) or Cl ions (Yelon *et al* 1975). Each Co^{2+} ion has seven 3d electrons, and so Hund's rules give the electronic ground state as ^4F. In an octahedral field this state is split into a singlet and two triplets (Abragam and Pryce 1951) with the Γ_4 triplet having the lowest energy. This state has the same symmetry as triplet p states and so the states within the Γ_4 ground state can be described with an effective orbital angular momentum $l = 1$, and the matrix elements of $\boldsymbol{L}$ within the ground state are given by $\alpha \boldsymbol{l}$ where $\alpha = -3/2$ in the absence of mixing with the higher energy states, and when the mixing is included $\alpha \sim -1.42$ (Griffiths 1961).

The distortions of the crystal field from full octahedral symmetry are orthorhombic in the case of CoF_2 as discussed by Gladney (1966), and by Cowley *et al* (1973). The Hamiltonian is given by

$$H = \sum_i H_i + H_{ex} \tag{1}$$

where the single-ion term is given for the ith ion by

$$H_i = \Gamma_z(l_z^2(i) - 2/3) + \Gamma_x(l_x^2(i) - l_y^2(i)) + \lambda \boldsymbol{l}(i) \cdot \boldsymbol{S}(i) + H_m S_z(i) \tag{2}$$

while the tetragonal and rhombic crystal-field parameters are Γ_z and Γ_x, the spin–orbit parameter is λ and H_m is the molecular field

$$H_m = 2 \sum J_r \langle S_z(r) \rangle \tag{3}$$

with J_r the exchange interaction between the rth nearest neighbours, where the sum is over all the neighbours. The spin direction z is the ordering direction of the magnetic moments.

The term H_{ex} in equation (1) is the part of the exchange interactions not included in the molecular-field interactions:

$$H_{ex} = \sum_{ij} J_{ij} \boldsymbol{S}(i) \cdot \boldsymbol{S}(j) - \sum_i H_m \langle S_z(i) \rangle. \tag{4}$$

In $CsCoCl_3$ the surroundings of each Co ion are of trigonal symmetry and this produces an axial crystal field (Nagler *et al* 1983). The Hamiltonian is then of the same form as for CoF_2 (equations (1)–(4)) except that the rhombic term, Γ_x, is absent.

In the case of CoF_2 the values of the parameters were deduced by Cowley *et al* (1973), from optical measurements, neutron measurements and spin resonance giving $\Gamma_z = -38.05$ meV, $\Gamma_x = -55.83$ meV, $\lambda = 28.54$ meV and $H_m = 4.55$ meV. The resulting

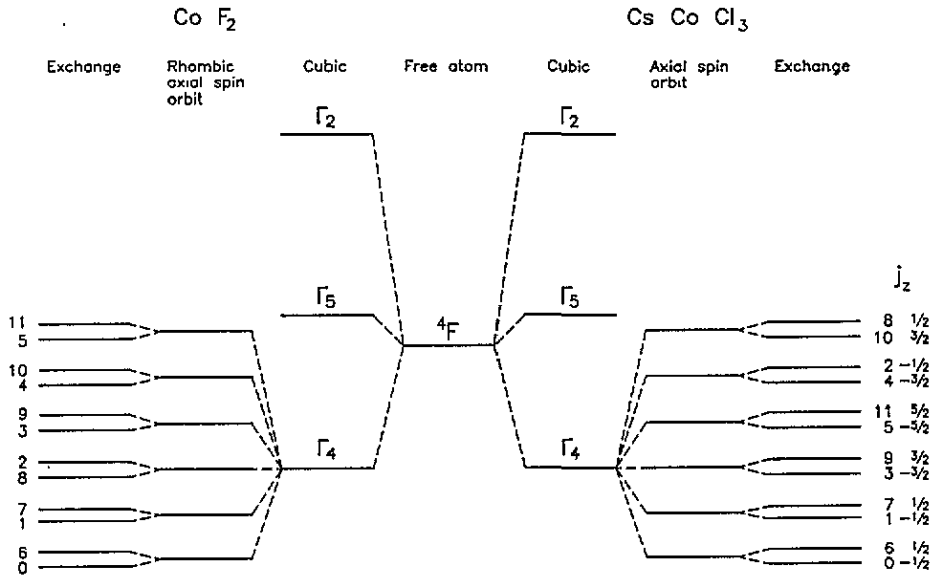

Figure 1. Energy levels of the Co^{2+} ion in CoF_2 and $CsCoCl_3$.

twelve energy levels ($l = 1, S = 3/2$) are then illustrated schematically in figure 1, while the resulting eigenvectors of the Hamiltonian matrix give the coefficient in the expansion of the pth wavefunction in the form

$$|\Psi_p\rangle = \sum C_p(l_z, S_z)|l_z S_z\rangle. \tag{5}$$

The resulting energies and coefficients are listed in table 1, where it is seen that the eigenstates fall into two groups having components of $j_z = l_z + S_z = 5/2, 1/2, -3/2$ or $3/2, -1/2, -5/2$.

Table 1. Wavefunctions of energies of Co ions in CoF_2.

Level	Energy (meV)						
		$\|1\,1/2\rangle$	$\|1\,-3/2\rangle$	$\|0\,3/2\rangle$	$\|0\,-1/2\rangle$	$\|-1\,1/2\rangle$	$\|-1\,-3/2\rangle$
0	0	0.171	0.805	−0.045	−0.332	0.294	0.361
1	23.4	−0.549	0.354	0.174	0.155	0.338	−0.195
2	102.5	−0.511	−0.083	0.577	−0.490	0.338	−0.212
3	137.7	0.064	−0.135	0.529	0.533	0.293	0.572
4	159.4	0.318	0.405	0.429	0.357	−0.041	−0.649
5	180.0	−0.551	0.193	−0.413	0.469	0.483	−0.194
		$\|1\,3/2\rangle$	$\|1\,-1/2\rangle$	$\|0\,1/2\rangle$	$\|0\,-3/2\rangle$	$\|-1\,3/2\rangle$	$\|-1\,-1/2\rangle$
6	7.9	0.255	0.549	−0.355	−0.117	0.595	0.375
7	24.3	−0.314	0.511	0.017	−0.164	−0.164	0.449
8	96.8	−0.149	0.396	−0.378	0.682	−0.111	−0.449
9	138.2	−0.406	−0.149	−0.649	−0.553	0.001	−0.292
10	164.5	−0.652	−0.317	−0.058	0.378	0.307	0.483
11	180.0	−0.473	0.397	0.554	−0.214	0.358	−0.371

Table 2. Energies and wavefunctions of Co ions in $CsCoCl_3$.

	Level	Energy (meV)			
(a) $j_z = -1/2$			$\|1\,-3/2\rangle$	$\|0\,-1/2\rangle$	$\|-1\,+1/2\rangle$
	0	0	−0.894	0.361	−0.265
	1	39.9	0.379	0.296	−0.877
	2	138.9	0.238	0.885	0.401
(b) $j_z = -3/2$			$\|0\,-3/2\rangle$	$\|-1\,-1/2\rangle$	
	3	53.2	−0.537	0.844	
	4	127.7	−0.844	−0.537	
(c) $j_z = -5/2$				$\|-1\,-3/2\rangle$	
	5	96.3		1	
(d) $j_z = 1/2$			$\|1\,-1/2\rangle$	$\|0\,1/2\rangle$	$\|-1\,3/2\rangle$
	6	12.8	0.481	−0.424	0.767
	7	39.9	0.799	−0.147	−0.582
	8	143.9	0.360	0.894	0.268
(e) $j_z = 3/2$			$\|1\,-1/2\rangle$	$\|0\,3/2\rangle$	
	9	62.2	0.878	−0.479	
	10	142.4	0.479	0.878	
(f) $j_z = 5/2$			$\|1\,3/2\rangle$		
	11	114.1	1		

The situation is similar but less complex in the case of $CsCoCl_3$ because the absence of the rhombic term means that j_z is a good quantum number. Consequently, there is one state with $j_z = 5/2$, and another with $j_z = -5/2$, two states each with $j_z = \pm 3/2$ and three states each with $j_z = \pm 1/2$. A schematic diagram for the energy levels is shown in figure 1, and the values of the energy levels and coefficients $C_p(l_z, S_z)$ listed in table 2, from calculations based on the values of the crystal-field and spin–orbit parameters deduced from the experimental results described below.

2.2. *The scattered neutron intensity*

The magnetic neutron scattering intensity for unpolarized neutrons is given by (Marshall and Lovesey 1971)

$$\frac{\mathrm{d}^2\sigma}{\mathrm{d}\,\Omega\,\mathrm{d}E} = b_{\mathrm{m}}^2 \frac{k}{k_{\mathrm{i}}} |f(Q)|^2 \sum \left(\delta_{\alpha\beta} - \frac{Q_\alpha Q_\beta}{Q^2}\right) T_{\alpha\beta}(Q, \omega) \tag{6}$$

where ω is the frequency transfer, Q is the wavevector transfer, b_{m} is the magnetic scattering length and $f(Q)$ is the form factor. The correlation function is given by

$$T_{\alpha\beta}(Q, \omega) = \sum_{\mathrm{fg}} p_{\mathrm{g}} \langle \mathrm{g}|M_\alpha(Q)|\mathrm{f}\rangle \langle \mathrm{f}|M_\beta(-Q)|\mathrm{g}\rangle\, \delta(E_{\mathrm{g}} - E_{\mathrm{f}} - \hbar\omega) \tag{7}$$

where |g⟩ and |f⟩ are the initial and final states of the system with energies E_g and E_f and the initial state has probability p_g. Within the dipole approximation the operator $M(Q)$ is given by

$$M(Q) = \sum (L(i) + 2S(i)) \exp(iQ \cdot R(i)). \tag{8}$$

The intensity of the inelastic scattering from the ground state to an excited state, f, is then proportional to

$$|\langle g|L_\perp + 2S_\perp|f\rangle|^2 \tag{9}$$

where $L_\perp$ and $S_\perp$ are the components of angular and spin momentum perpendicular to the wavevector transfer. $CsCoCl_3$ has a ground state with $j_z = -1/2$ so excited states |f⟩ with $j_z = -1/2$ can be produced when $L_\perp$ and $S_\perp$ have components along z while, if they have components along x and y, states with $j_z = 1/2$ and $-3/2$ can be produced. In contrast, in CoF_2, transitions within one set of states are produced by components along z and transitions to the other set of states are produced by the x and y-components.

3. Experiments and results

3.1. The experiments

The neutron scattering measurements were performed with the time-of-flight direct-geometry spectrometer, HET, on the pulsed neutron source ISIS at the Rutherford Appleton Laboratory (Taylor *et al* 1987). The chopper is phased to the pulse source so as to produce pulses of nearly monoenergetic neutrons and in these experiments the incident neutron energy was chosen in the range between 80 and 450 meV. There are two banks of detectors: a low-angle bank covering angles between 3° and 7° at a distance of 4 m from the sample and a larger-angle bank, 10° to 30° , at a distance of 2.5 m. The data from the small-angle detector were mostly added together while those from the larger-angle bank were added in 4° blocks.

The CoF_2 sample was a large single crystal with a volume of 8 cm^3, while the $CsCoCl_3$ crystal was a cylinder of length 3.5 cms and a volume of 4 cm^3, and both were aligned so that either the crystallographic a- or c-axes could be aligned parallel to the incident neutron beam. The crystals were mounted on a closed-cycle refrigerator and the temperature of the samples held at 15 ± 2 K. this is well below the magnetic ordering temperature of CoF_2, 36 K, and of $CsCoCl_3$, 21 K.

The time-of-flight spectra were converted to energy distributions, corrected for the energy dependence of the detector efficiency, and then plotted against the energy transfer as shown in figures 2 and 3 for CoF_2 and figure 4 for $CsCoCl_3$. The results shown in figures 2 and 4 were obtained with the c-axis parallel to the incident beam when, for the low-angle bank, the wavevector transfer is largely parallel to the c-axis except for at very low energy transfers. Consequently, the peaks observed in figures 2 and 4 arise from transitions associated with the operators $L_x + 2S_x$ and $L_y + 2S_y$. Similar experiments, such as that shown in figure 3, were performed with the a-axis parallel to the incident beam. In this orientation the scattering observed arises from both the transverse operators, $L_x + 2S_x$ and $L_y + 2S_y$, and the longitudinal operator, $L_z + 2S_z$. Hence by comparing the results for the two orientations information can be obtained about the transitions produced by the different operators.

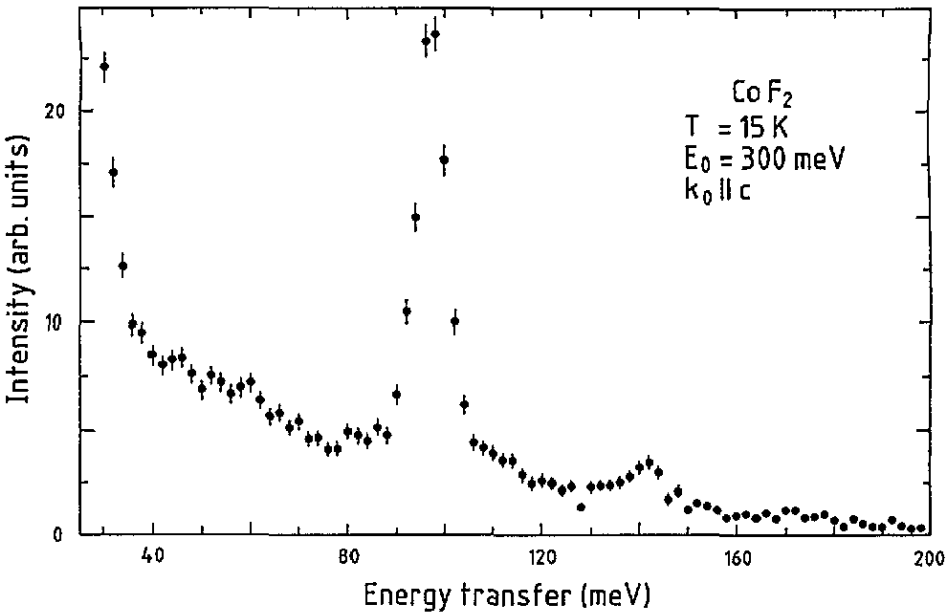

Figure 2. The energy distribution of scattered neutrons in the low-angle bank of detectors from CoF_2 with $k_0 \| c$.

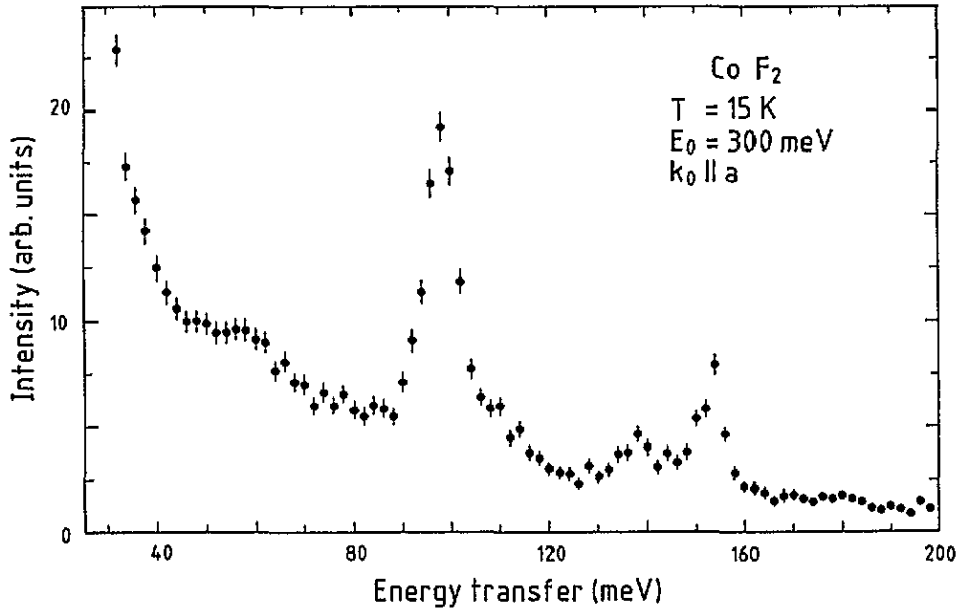

Figure 3. The energy distribution of scattered neutrons in the low-angle bank of detectors from CoF_2 with $k_0 \| a$

3.2. Results for CoF_2

The results obtained for CoF_2 with the **c**-axis parallel to an incident beam and an incident energy of 300 meV are shown in figure 2. There are peaks at energies of 96 and 141 meV,

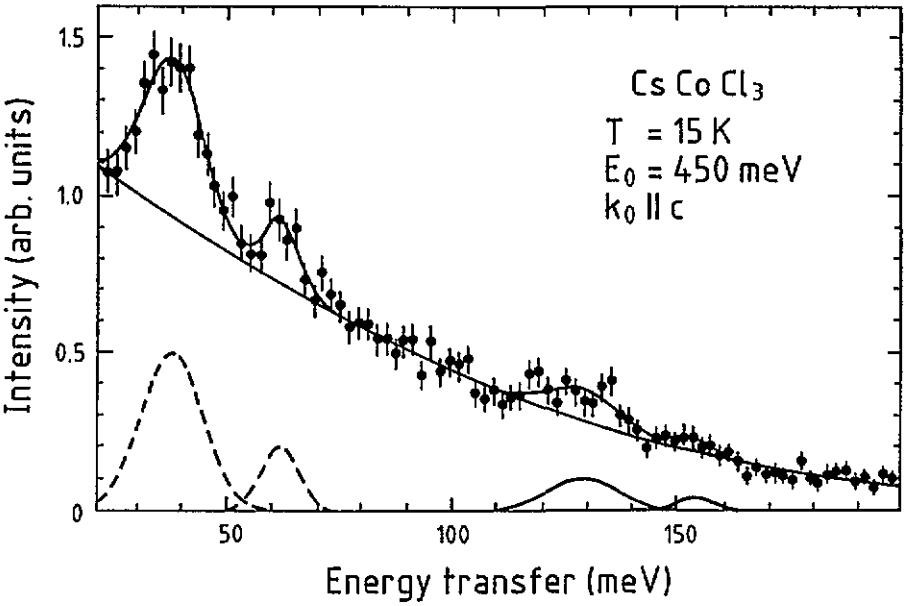

Figure 4. The energy distribution of scattered neutrons in the low-angle bank of detectors from $CsCoCl_3$. The line shows a fit to Gaussian peaks and a background.

and similar measurements with a lower incident energy give peaks at 8 and 24 meV. These low-energy peaks were, however, studied in detail by Martel *et al* (1968) and so this experiment was not designed to study them further. The energies of the peaks are listed in table 3 and they correspond to excitations from the ground state (0 of table 1) to the states labelled 6–11. Clearly the energies correspond well with the calculated energies of states 6–9. Also shown in table 3 are the intensities of the different excitations normalized to the intensity of the excitation at 96 meV, and these are compared with calculations of the intensities from the wavefunctions in table 1 and the symmetric form factor of Watson and Freeman (1961). The results from the experiment and the theory are in agreement for both the energies and the intensities, and further show that the intensities expected for the transitions to the levels 10 and 11 are so small as to be unobservable in this experiment.

Table 3. Energies and intensities observed with $k_i \| c$ in CoF_2.

	Energy (meV)		Intensity	
Level	Experiment	Theory	Experiment	Theory
6	8.0 ± 0.5	7.8	—	—
7	23.9 ± 1.0	24.3	2.6 ± 0.3	2.8
8	96.4 ± 2.0	96.8	1	1
9	141 ± 3.0	138.2	0.19 ± 0.04	0.18
10	—	164.5	< 0.05	0.05
11	—	180.0	< 0.05	0.00

The results shown in figure 3 were obtained with the a-axis parallel to the incident beam. The spectra are clearly different especially because of the presence of a new peak at 153 meV, and possibly a shoulder at 105 meV in the side of the peak at 98 meV. In

Table 4. Energies and intensities observed with $k_I \| a$ in CoF_2.

	Energy (meV)			Intensity	
Level	Experiment	Theory	Johnson	Experiment	Theory
1		23.4			2.4
	24.2 ± 0.1		18.9	3.2 ± 1.0	
7		24.3			2.0
8	98.0 ± 2.0	96.8		1	1
			97.6		
2	105.0 ± 5	102.6		0.13 ± 0.03	0.14
3		137.7			0.08
	138.1 ± 3.0		135.4	0.21 ± 0.05	
9		138.2			0.17
4		159.4		0.25 ± 0.03	0.31
	153.1 ± 3.0		155.8		
10		164.5		< 0.05	0.05
5		180.0		< 0.05	0
			173.5		
11		180.0		< 0.05	0

table 4 we collect together all the high frequencies observed in this geometry together with the intensities normalized to that of the 98 meV peak. Clearly in view of the uncertainties caused by the large crystal, multiple scattering and absorption, the agreement between experiment and theory is very satisfactory. Also shown in table 4 are the energies observed by Johnstone *et al* (1964) for dilute Co in MgF_2. Their energies are on average expected to be 5 meV lower in energy than ours due to the absence of the molecular field in the dilute system.

Further evidence that the scattering is magnetic in origin is provided by the data obtained using the $2\frac{1}{2}$ m bank. As shown in figure 5 the intensities of the peaks decrease with increasing angle, as expected for magnetic scattering governed by a form factor. In detail however, the decrease in intensity with increasing angle is less rapid than expected from the isotropic part of the form factor, as shown in figure 6. Unfortunately, the detailed theory of the intensity of the scattering in systems with different orbital wavefunctions for different states has not been worked out. The effects of the different wavefunctions will lead to differing and anisotropic form factors for the different transitions. In view of this it is surprising that the results for the different transitions are so similar. In figure 6 we also show the form factor calculated from the sum of the isotropic $\langle j_0 \rangle$ and anisotropic $\langle j_2 \rangle$ parts of the form factor (Watson and Freeman 1961). Clearly the anisotropic terms decrease the wavevector dependence and can be used to explain the observed effects, but further work is needed, in the form of a detailed calculation for CoF_2, to establish the detailed wavevector dependence of the scattering.

3.3. Results for $CsCoCl_3$

The scattered intensity from $CsCoCl_3$ is shown in figure 4 with an incident neutron energy of 450 meV and the *c*-axis parallel to the incident beam. The results were fitted to four Gaussian peaks and a smooth background, and gave peaks at 37, 60, 128 and 153 meV as listed in table 5. Similar results were obtained with incident neutron energies of 80 and 250 meV and showed also a low-energy excitation at 13 meV. This is in good accord

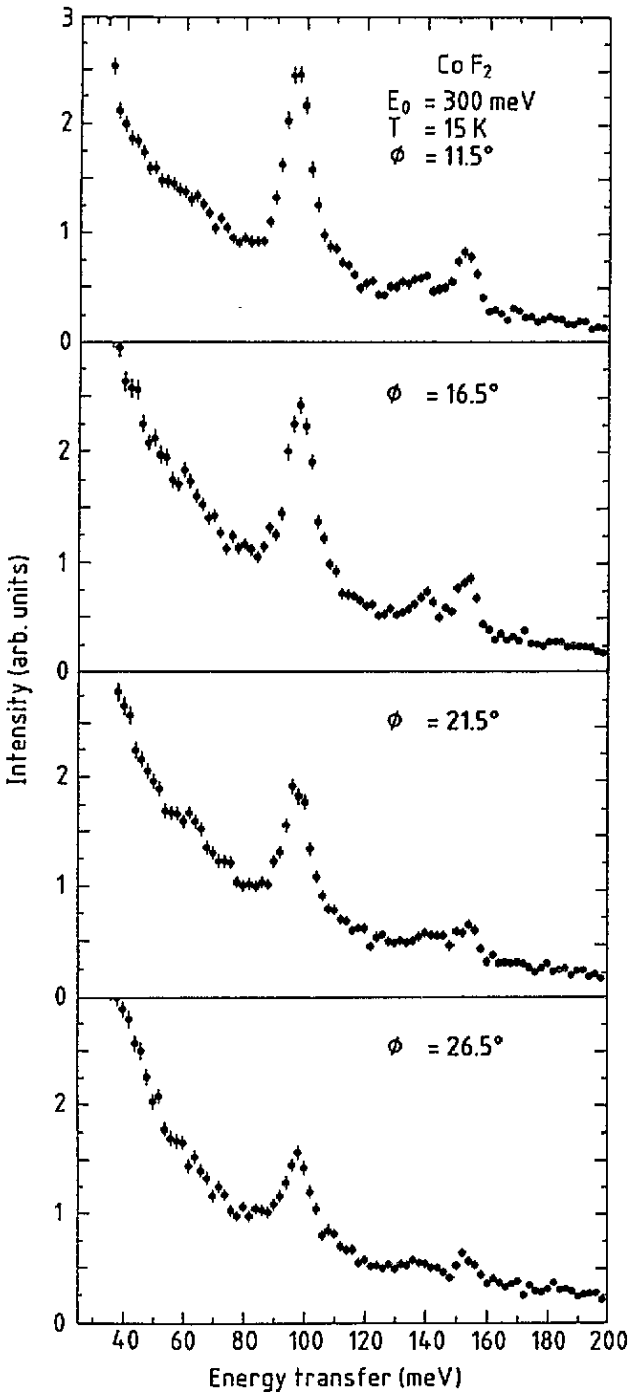

Figure 5. The energy distributions of the scattered neutrons at increasing angles of scattering in the high-angle bank of detectors.

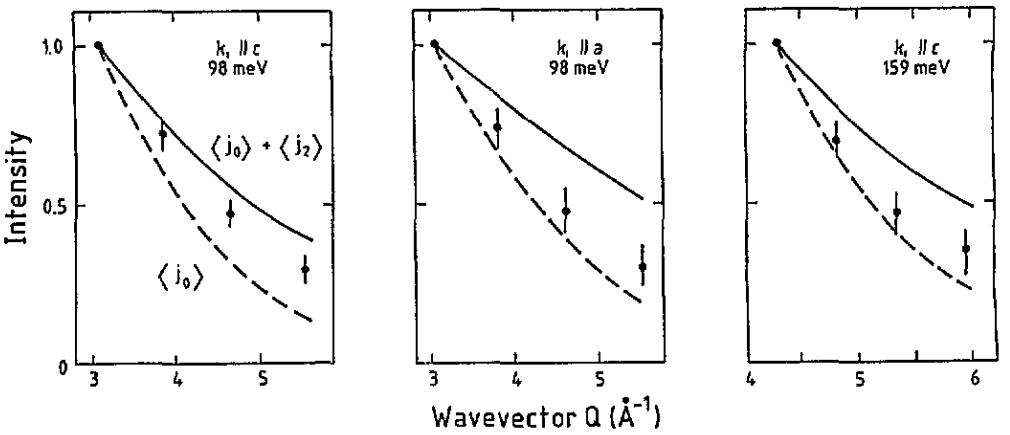

Figure 6. The intensity of the transitions in CoF_2 as a function of wavevector transfer compared with the form factor calculations of Watson and Freeman (1961) showing the j_0 (dotted line) and $j_0 + j_2$ calculations (solid lined).

with the low-energy excitations studied by Tellenbach and Arend (1977), Yoshizawa *et al* (1981) and by Nagler *et al* (1983) while Buyers *et al* (1980) have also observed the level at 37 meV. Similar experiments were performed with the *a*-axis parallel to the incident beam and the results obtained were very similar to those for the c-axis. This is presumably because transitions to states 1 and 7 have very similar energies while the highest-energy excitations have very low intensities; see table 5. As expected the intensities of the peaks decreased with increasing angle in the high-angle bank showing that they arise from magnetic scattering. Also shown in table 5 are the frequencies of the strongest peaks observed in the Raman scattering measurements of Johnstone *et al* (1982) at 6 K. They are in generally good agreement with our results, given the difficulty of distinguishing one- and two-magnon processes in the Raman scattering, apart from the frequency at 105 meV.

Table 5. Energies and intensities observed in $CsCoCl_3$. The obseverations marked * were taken with the *a*-axis parallel to k_I and the others with the *c*-axis parallel to k_I.

Exited state	Observed frequencies (meV)	Raman frequencies (meV)	Calculated (meV)	(Matrix element)^2
6	12.96 ± 0.08		12.8	2.86
7	37.0 ± 0.2		39.9	1.98
		37.2		
1	37.4 ± 0.2*		39.9	3.84
3	60.5 ± 1.0	64.0	53.2	2.48
	60.4 ± 1.6*	69.4		
		105.5		
4	128.3 ± 1.2	123.9	127.7	0.65
	130.2 ± 1.6*	133.8		
2	153.4 ± 2.5	142.9	138.9	0.13
		147.5		
8	—		143.9	0.0054

In contrast to the case for CoF_2 our observed frequencies are not consistent with the parameters proposed earlier (Nagler *et al* 1983). When the crystal-field parameters are

deduced from the four strongest neutron scattering transitions, the crystal-field parameter Γ_z, spin–orbit parameter, λ, and the nearest-neighbour exchange parameter J are $\Gamma_z = 51.3 \pm 1.0$ meV, $\lambda = 27.6 \pm 0.5$ meV and $J = 2.42 \pm 0.1$ meV. The value of λ is close to that of the free-ion value with the appropriate orbital reduction factors, and to the average of the anisotropic spin–orbit parameter deduced by Johnstone *et al* (1982). The crystal-field parameter, Γ_z, is substantially smaller than that obtained earlier, 165 meV, but fairly close to that obtained by Johnstone *et al* (1982), 56 meV. The exchange parameter that we obtain is close to that of Nagler *et al* (1983) who performed the most detailed neutron scattering measurements of the lowest excitation. Our final parameters were used to calculate the frequencies, eigenvectors and intensities given in tables 2 and 5. The model does not give a good description of the highest-energy peak, but this is very weak and further experiments are needed to clarify the energy of this excitation. The observed intensities are rather uncertain due to the irregular shape of the sample but they are generally consistent with the calculated matrix elements and the form factor of Watson and Freeman (1961).

One unexpected feature of the results was that the scattering depended on the azimuthal angle. The low-angle detector bank has five sections separated by an azimuthal angle of 72°: one of the segments is horizontal, two are at 72° and two are at 144°. The spectra were different from the different segments, near 38 meV energy transfer, and some of these spectra clearly showed two peaks. These effects arise from the dispersion of the frequency of the excited state because the different spectra corresponded to different wavevectors along the chain direction.

The dispersion relation for the excitations to level one can be calculated using the pseudo-boson techniques:

$$\hbar\omega_1(q) = \left(E_1\left(E_1 + 2d^2 J(q)\right)\right)^{1/2} \tag{10}$$

where E_1 is the molecular-field energy $J(q) = 2J\cos q$ and d is the matrix element $\langle 0|S_z|1\rangle$. Using the model given in table 1, this dispersion was calculated using the value of J obtained above and d calculated from the wavefunctions of table 2, and the result is shown in figure 7. The dispersion for level 7 was also obtained from

$$\hbar\omega_7(q) = \left(E_7^2 - (cJ(q))^2\right)^{1/2} \tag{11}$$

where c is the matrix element $\langle 0|S_+|7\rangle$. Clearly within the very considerable errors the dispersion of the excitations 1 and 7 can account for the results shown in figure 7. Two peaks are resolved when the energies of levels 1 and 7 are sufficiently different but only one when they are close in energy.

The dispersion of the excitations associated with higher energies was calculated and found to be negligible.

4. Conclusion

The main conclusion of our work is that neutron scattering techniques can now be used to study the crystal-field excitations in the 3d transition metal ions. The development of spallation sources has provided neutrons of sufficiently high energy to allow measurement of excitations in the energy range 100–1000 meV.

In the case of CoF_2 we have been able to identify all but the highest-energy excitations, and calculations show that these are expected to have very low intensities. The energies are in very good agreement with calculations based on earlier measurements of CoF_2 and dilute Co ions in MgF_2, and essentially show that the technique is reliable.

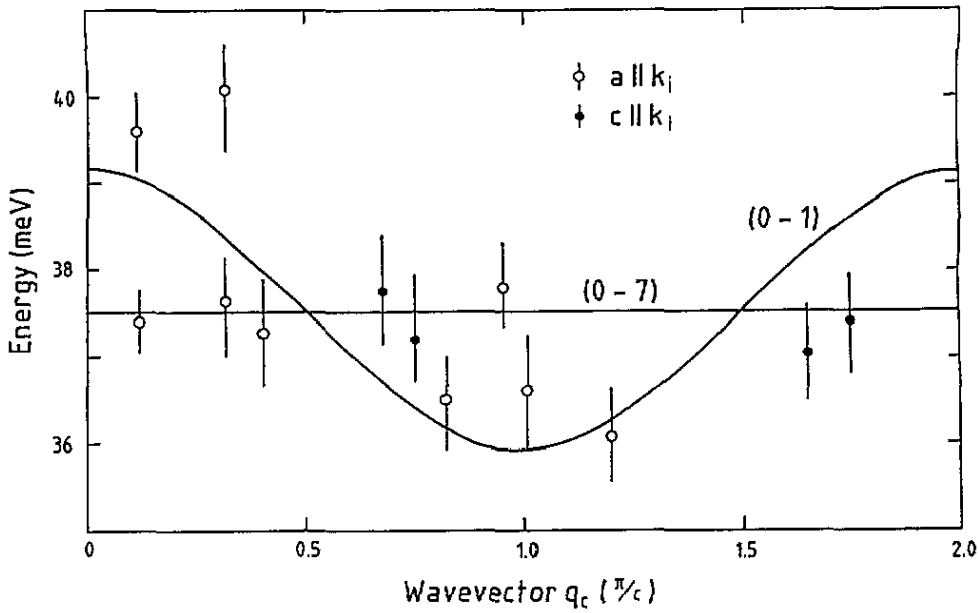

Figure 7. The dispersion of the excitation at 38 meV in $CsCoCl_3$ as observed experimentally and calculated as described in the text.

The crystal-field parameters for $CsCoCl_3$ were less well known, and our results are inconsistent with some previous estimates. We have been able to study the five accessible high-energy excitations and to deduce a new crystal-field model. The new model has been used to calculate the anistropy of the exchange interaction when Heisenberg exchange interactions between real spins are projected into the two lowest states. The results give only 40% of the dispersion observed in the neutron scattering measurements (Tellenbach and Arend 1977, Yoshizawa *et al* 1981, Nagler *et al* 1983). This suggests that the interaction between real spins in $CsCoCl_3$ is more complex than a simple Heisenberg form.

We have also observed evidence for the dispersion of the excited states in $CsCoCl_3$ and shown that this is qualitatively consistent with theory, and finally in CoF_2 we have observed evidence for the failure of the calculated isotropic form factor in explaining the intensity of the excited states.

Acknowledgments

We are grateful to R Ward who grew an excellent crystal of $CsCoCl_3$ and to Z Bowden and A Taylor for help with the experiment. Financial support was provided by Science and Engineering Research Council who provided TBN with a studentship and SN with a Visiting Fellowship.

References

Abragam A and Pryce M H L 1951 *Proc. R. Soc.* A **206** 173
Buyers W J L, Yamanaka Y, Nagler S E and Armstrong R L 1980 *Solid State Commun.* **33** 857
Cowley R A, Buyers W J L, Martel P and Stevenson R W H 1973 *J. Phys. C: Solid State Phys.* **6** 2997
Gladney H M 1966 *Phys. Rev.* **146** 253
Griffiths J S 1961 *The Theory of Transition Metal Ions* (Cambridge: Cambridge University Press)

Johnstone I W and Dubicki L 1980 *J. Phys. C: Solid State Phys.* **13** 4531
Johnstone I W, Jones G D and Lockwood D J 1982 *J. Phys. C: Solid State Phys.* **15** 2043
Johnson L F, Dietz R E and Guggenheim 1964 *Appl. Phys. Lett.* **5** 21
Marshall W and Lovesey S W 1971 *Theory of Thermal Neutron Scattering* (Oxford: Oxford University Press)
Martel P, Cowley R A and Stevenson R W H 1968 *Can. J. Phys.* **46** 1355
Nagler S E, Buyers W L J, Armstrong R L and Briat B 1983 *Phys. Rev.* B **27** 1784
Osborn R, Baker E, Lovesey S W and Taylor A D 1991 *Handbook of Physics and Chemistry of Rare Earths* vol 14 (Amsterdam: North-Holland)
Stout J W and Reed S A 1954 *J. Am. Chem. Soc.* **76** 3279
Taylor A D, Boland B C, Bowden Z and Jones T J L 1987 *Rutherford-Appleton Laboratory Report No* 87-012
Tellenbach U and Arend H 1977 *J. Phys. C: Solid State Phys.* **10** 1311
Yelon W B, Cox D E and Eibschultz M 1975 *Phys. Rev.* B **12** 5007
Yoshizawa H, Hirakawa K, Satija S K and Shirane G 1981 *Phys. Rev.* B **23** 2298
Watson R E and Freeman A J 1961 *Acta Crystallogr.* **14** 27